RESEARCH ARTICLE

ROCK Inhibitor Y-27632 Promotes Human Retinal Pigment Epithelium Survival by Altering Cellular Biomechanical Properties

Y. Ni[1,#], Y. Qin[1,#], Z. Fang[2] and Z. Zhang*[,1]

[1]State Key Laboratory of Ophthalmology, Zhongshan Ophthalmic Center, Sun Yat-sen University, Guangzhou 510060, China; [2]Zhongshan School of Medicine, Sun Yat-sen University, Guangzhou 510080, China

Abstract: *Purpose*: Dysfunction or death of retinal pigment epithelial (RPE) cells is a common pathogenesis of various types of retinal degenerative diseases. Recent reports indicated that ROCK pathway inhibitors regulate cell proliferation or apoptosis in a cell-type-dependent manner. Here, we aim to investigate the effect of ROCK inhibitor Y-27632 on the human retinal pigment epithelium (RPE) *in vitro*.

Methods: Cell proliferation and apoptosis were analyzed by CCK-8 and flow cytometry respectively. Cell proliferation markers were detected by immunofluorescence and western blot. Cell morphology was evaluated using scanning electron microscopy. The topography and biomechanical properties of living cells were assessed using atomic force microscope (AFM). In addition, cytoskeleton and epithelial-mesenchymal transition (EMT) markers were detected by western blot and immunofluorescence.

Results: 30µM Y-27632 significantly promoted cell proliferation and decreased apoptosis. Compared with control group, human retinal pigment epithelial cell line ARPE-19 cells treated with 30µM Y-27632 exhibited significantly decreased cytomembrane roughness (Ra: 41.04±1.63nm *vs*. 24.41±0.75nm, *P*<0.01; Rq: 51.56±2.03nm *vs*. 30.81±0.95nm, *P*<0.01) and increased elasticity modulus (16.66±0.83KPa *vs*. 32.55±1.48KPa, *P*<0.01). In addition, the inhibition of ROCK activity by Y-27632 caused cell elongation and reorganization of microfilaments and microtubules of cytoskeletons.

Conclusion: Taken together, our data demonstrated that Y-27632 could alter biomechanical properties and reorganized cytoskeletons to promote RPE cell survival. These results are an important step toward the future application of Y-27632 in retinal degenerative diseases.

1. INTRODUCTION

The retinal pigment epithelium (RPE) is located between the neurosensory retina and the choriocapillaris in the healthy eye. These monolayer cells are of vital importance to the maintenance and function of overlying rod and cone photoreceptors and, hence, for normal visual function [1, 2]. Dysfunction or death of RPE cells is a common pathogenesis of various types of degenerative eye diseases, including Stargardt's disease [3], retinitis pigmentosa (RP) [4], and age-related macular degeneration (AMD) [5], which is the major cause of irreversible blindness in the elderly worldwide. Although there were continuous attempts, many patients have no chance to restore vision. Recently, delaying/blocking the apoptosis of RPE cells has been suggested as an alternative approach to halt the progression of degenerative eye diseases [6-8].

The Rho-associated coiled-coil containing kinases (ROCK), believed as effectors of the RhoA small GTPase, participate in actomyosin cytoskeleton contraction and RhoA and RhoC activation [9-11]. Since then, the roles of ROCK have been widely recognized in some other aspects of cell behavior, such as cell proliferation, apoptosis and transformation [12]. Although the underlying mechanism has yet to be thoroughly revealed, recent reports indicated that the different roles of ROCK activation in apoptosis are highly dependent on cell type. ROCK activation contributes to cell survival in pancreatic stellate cells, airway epithelial cells, and glioma cells [13-15]. Whereas, ROCK specific inhibition of Y-27632, has

*Address correspondence to this author at the State Key Laboratory of Ophthalmology, Zhongshan Ophthalmic Center, Sun Yat-sen University, 54S Xianlie Road, Guangzhou 510060, China;
Tel: +86 182-0099-1688; Fax: +862087330415;
E-mail: zhangzhaotian@gzzoc.com

#These authors are equally contributed to this work.

been demonstrated as an effective inhibitor of apoptosis in embryonic stem cells [16, 17], cardiomyocyte [18, 19], and corneal endothelial cells in the eye [20]. Given the principal function of ROCK that mediated its downstream effects on actin organization, Y-27632 has been explored in some ocular diseases associated with the contractile activity of cells [21-26]. Nevertheless, its precise role in apoptosis-related degenerative eye diseases has yet to be established.

In this study, we aimed to determine whether ROCK inhibitor Y-27632 would promote proliferation or block apoptosis in human retinal pigment epithelium, and be helpful for the survival of RPE cells *in vitro*. Since cellular mechanical properties are sensitive indicators for indicating cell states [27-29], we also analyzed the influence of Y-27632 on biophysical properties in alive RPE cells by Atomic force microscopy (AFM). ROCK inhibitor Y-27632 has already been used clinically in cardiovascular therapies, suggesting that it is safe for use with the human body [30]. We expect that our study will be valuable in establishing a clinically applicable way to use Y-27632 in apoptosis-related degenerative eye diseases.

2. MATERIALS AND METHODS

2.1. Cell Culture and Treatment

Human retinal pigment epithelial cell line ARPE-19 cells were cultured in Dulbecco's modified Eagle's medium (DMEM; GIBCO, Grand Island, NY, USA) supplemented with 10% HyClone™ Fetal Bovine Serum (FBS; GE Healthcare Life Sciences Company, USA). After 24h incubation at 37°C and 5% CO_2 in a humidified incubator for cell adherent growth, ARPE-19 cells were treated with or without Y-27632 (Selleckchem Company, USA) for further experiments. Y-27632 was diluted in DMSO at a final concentration of 0.03% in the DMEM, which showed no detectable effect on cell proliferation and apoptosis.

2.2. Cell Proliferation Assay

Cell proliferation was assessed using Cell Counting Kit-8 (CCK-8; Dojindo, GMBH, EU). The cells were seeded in 96-well plates at the density of $5.0×10^3$ cells/well. After cell adherent growth, plates were washed twice with DMEM. Y-27632 was added to the medium to the final concentrations (0, 30μM). The cells were treated with or without Y-27632 for 24h, 36h or 48h. Subsequently, the cells were incubated with 10μL of the CCK-8 solution at 37°C for 2h in dark. The optical density (OD) values were determined using a 96-well microplate reader (Tecan Sunrise Reader, Switzerland) at 450nm.

2.3. Cell Apoptosis Assay

Flow cytometry reagents (Becton, Dickinson and Company, USA) were used according to the manufacturer's protocol. Briefly, ARPE-19 cells were trypsinized and collected in 100μL 1× binding buffer. Then the cells were incubated with the labeling solution (5μL Annexin V-APC and 5μL propidium iodide (PI)) for 20min in the dark. After that, each sample was diluted with 1×binding buffer to 500μL at the cell density of $1×10^6$/mL. The samples were analyzed by a flow cytometry (Beckman CytoFLEX S, Germany).

2.4. Scanning Electron Microscopy (SEM)

To assess morphology, ARPE-19 cells were seeded on chamber slides and treated with or without Y-27632. Each group was fixed in 2.5% glutaraldehyde-4% paraformaldehyde in PBS for 0.5h at room temperature. After dehydrated through a graded ethanol series (50%, 70%, 85%, 100%), specimens were dried in a CO_2 critical point dryer. Then the samples were sputter coated with gold and examined by an FEI QUANTA200 SEM.

2.5. Atomic Force Microscopy (AFM)

A Dimension Fastscan with ScanAsyst™ AFM (Bruker, Santa Barbara, CA) was used to analyzed biophysical changes in a single living cell [31-35]. The pyramidal tip of silicon nitride cantilevers (nominal spring constant k=0.01N/m, tip radius 20.0nm, tip half angle 18.0°, MLCT-C, Bruker, USA) was used for the contact mode of AFM. This experiment was performed as described previously [35]. The cells were imaged over an area of $20×20μm^2$ with a resolution of 128×128 pixels. NanoScope Analysis (Bruker, USA) was used to calculate cell elasticity values and roughness values. The Young's modulus was calculated using Hertz model, which was selected from 10-12loci (2μm×2μm) on each cell [33].

2.6. Immunofluorescence

In short, the cells were washed with PBS buffer and fixed using 4% paraformaldehyde for 30min at RT. After permeabilizing in PBS containing 0.1% Triton X-100, the cells were blocked with 1% bovine serum albumin (BSA) for 1h. Then, the cells were incubated with primary antibodies and FITC-conjugated antibody (1:100; Cell Signaling Technology, Danvers, MA, USA). The CytoPainter Phalloidin-iFluor 488 reagent (1:100; Abcam, Cambridge, MA, USA) was used to label microfilaments (MFs) for 30min. Then, Hoechst33342 (1:1000; Abcam, Cambridge) was used to stain the cell nuclei for 30min. The images were taken using Zeiss LSM 800 microscope (LSM800, Zeiss, Germany). The sources of the primary antibodies are as follows: rabbit anti-β-tubulin antibody (1:50; Abcam), rabbit anti-Ki67 antibody (1:50; Abcam) and mouse anti-Vimentin (1:50; Abcam).

2.7. Western Blot

ARPE-19 cells were washed with PBS and then lysed in RIPA buffer supplied with protease. The BCA-100 Protein Quantitative Analysis Kit (Biocolor Bioscience & Technology Co. Ltd., Shanghai, China) was used to detect protein concentration. Samples were separated in 10% sodium dodecyl sulfate-polyacrylamide gel electrophoresis (SDS-PAGE) and

then transferred to polyvinylidene fluoride membranes (PVDF membranes; Millipore, MA, USA). 5% BSA was used to block nonspecific binding sites for 1h at RT. Then the PVDF membranes were incubated with primary antibodies and horseradish peroxidase (HRP)-conjugated secondary antibodies. The signals of each band were detected using an eECL Western Blot Kit (ComWin Biotech Co., Ltd, Beijing, China). The sources of the antibodies used are as follows: mouse anti-cyclin E1 (1:1000; Cell Signaling Technology), mouse anti-cyclin D1 (1:2000; Cell Signaling Technology), rabbit anti-P21 (1:2000; Cell Signaling Technology), mouse anti-α-SMA (1:1000; Abcam) , rabbit anti-E-cadherin (1:1000; Cell Signaling Technology) and mouse anti-β-actin (1:2000; Cell Signaling Technology).

2.8. Statistical Analysis

Statistical tests were conducted with SPSS 13.0. Student's *t* test was used to compare means between the control and the treatment group. Error bars represent standard deviation (SD). The level of statistical significance (*P* value) is indicated in the corresponding figure legends, *$P<0.05$, **$P<0.01$, ***$P<0.001$.

3. RESULTS

3.1. Y-27632 Promotes the Survival of ARPE-19 Cells

To investigate the effects of Y-27632 on cell growth. Cell proliferation of ARPE-19 cells was assessed with or without Y-27632 treatment. We evaluated cell proliferation marker Ki67 after 10μM Y-27632 and 30μM Y-27632 treatment for 48h. ARPE-19 cells

treated with 30μM Y-27632 showed more Ki67-positive cells (Fig. **1a**), indicating promoted cell proliferation. The CCK-8 assay was also performed. Consistently, 30μM Y-27632 treatment for 24h, 36h and 48h markedly increased cell proliferation, as the group treated with Y-27623 had significantly higher OD values than the untreated group (0.559±0.021 *vs.* 0.768±0.050 at 48h, *P*<0.001) (Fig. **1b**).

We next tested the effect of Y-27632 on cell apoptosis. After 48h of treatment with 30μM Y-27632, apoptosis of cells in both early and late phase was inhibited, and the data are shown in Fig. **2**.

To further understand the mechanism of cell cycle, we assessed the expression level of key cell cycle regulators. During a normal cell cycle, Rb was phosphorylated by cyclin D1/CDK6/CDK4 complex and cyclin E1/CDK2 complex to entering S phase. P21 could inhibit CDK2 activation [36]. We found that treated with 30μM Y-27632 for 48h significantly increased the expression levels of cyclin E1, cyclin D1 and downregulated the expression level of P21 (Fig. **3**). These data suggested that 30μM Y-27632 promotes cell cycle progression and inhibits apoptosis in ARPE-19 cells.

3.2. Y-27632 Modulates ARPE-19 Cells Phenotype

Knowing that Y-27632 strongly promoted cell proliferation, we next characterized the phenotype of ARPE-19 cells. The untreated ARPE-19 cells were round, or slightly elongated and remained tightly attached to each other and had a typical polygonal appearance (Fig. **4a**). However, the ROCK inhibitor Y-27632 caused morphological changes in the cells. The treated cells became elongated in shape (Fig. **4b**).
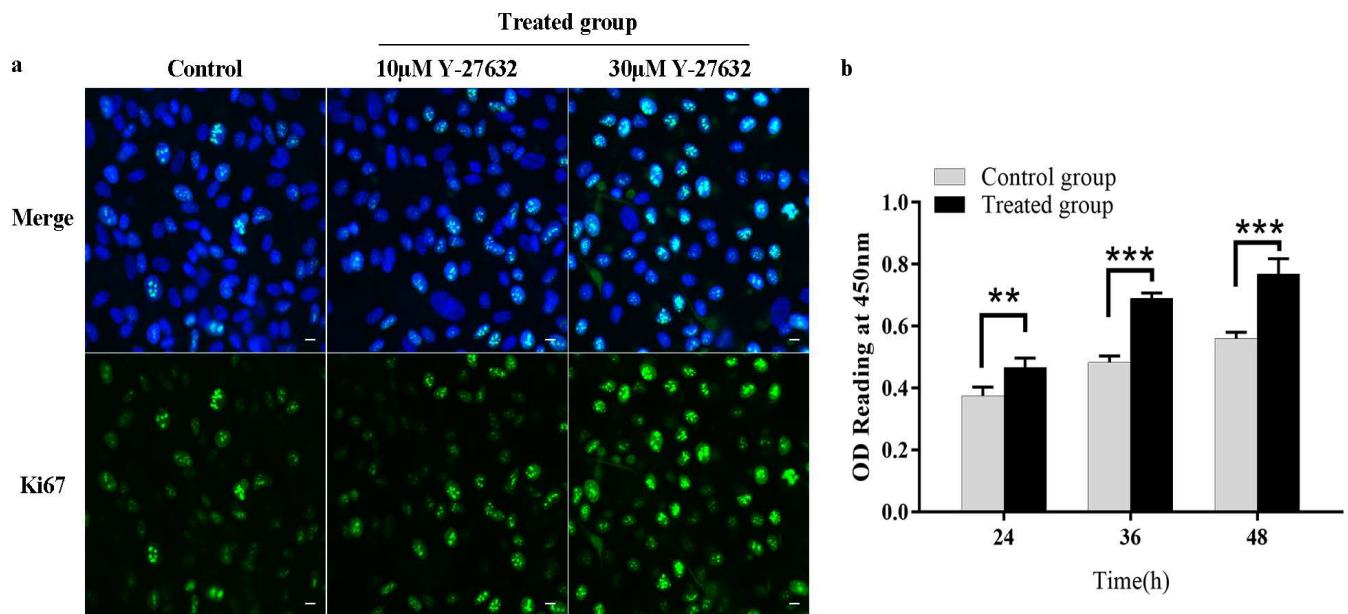
Fig. (1). The effect of ROCK inhibitor Y-27632 on cell proliferation. (**a**) ARPE-19 cells were treated with 10μM/30μM Y-27362 for 48h. Then cells were probed for Ki67 (green) and Hoechst (blue). Scale bar: 10μm. (**b**) ARPE-19 cells were treated with 30μM Y-27362 for 24h, 36h and 48h. Cell proliferation was analyzed by CCK-8 assay. Data represent the mean ± S.D. **P<0.01, ***P<0.001, n=3.
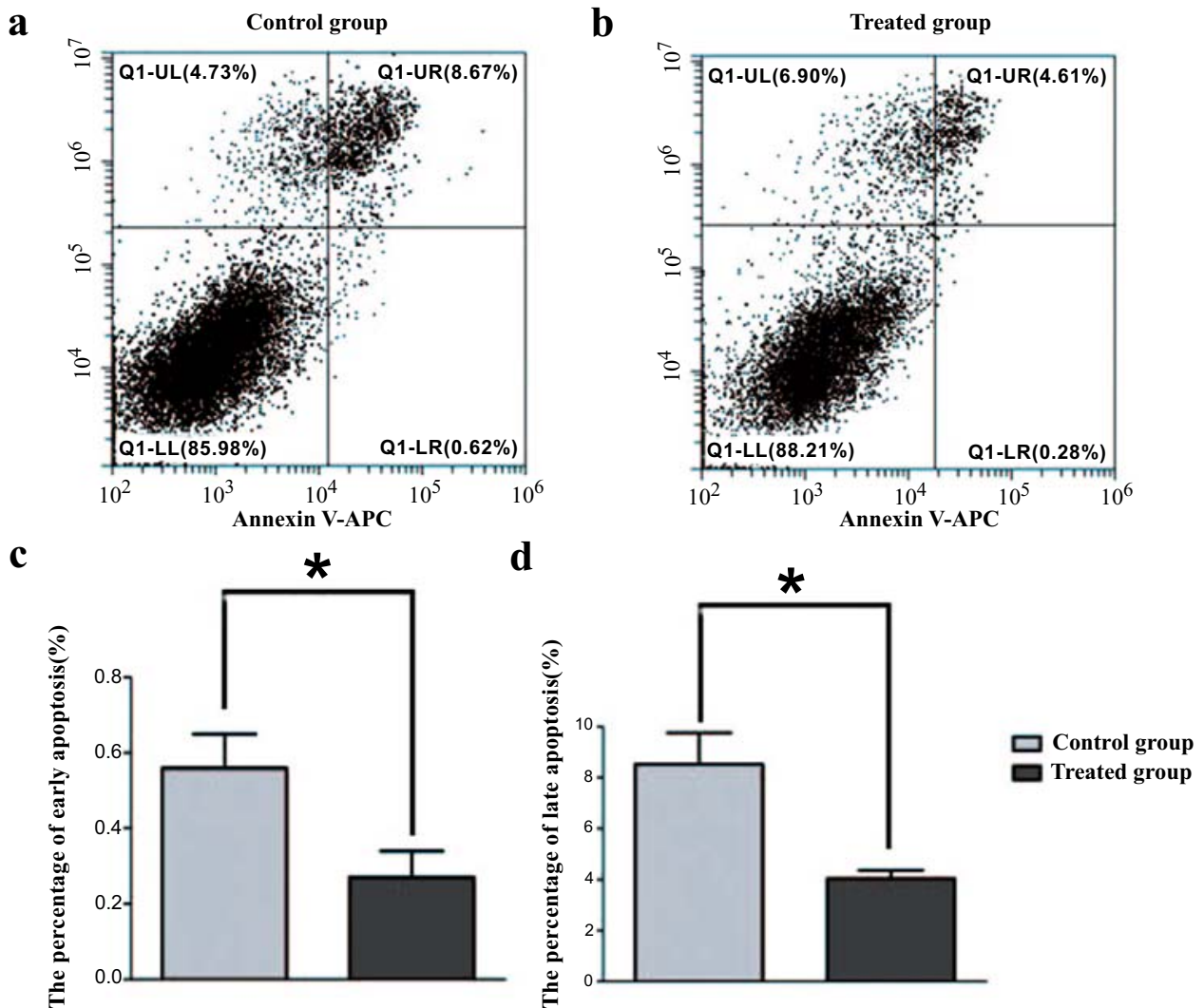
Fig. (2). The effect of ROCK inhibitor Y-27632 on cell apoptosis. ARPE-19 cells were treated with 30μM Y-27362 for 48h. Cell apoptosis analysis of control group (**a**) and 30μM Y-27362 treated group (**b**). Results of cellular early apoptosis and cellular late apoptosis after 48 h of treatment (**c-d**). Data represent the mean ± S.D. *P<0.05, n=3.

3.3. Y-27632 Alters Biomechanical Properties of ARPE-19 Cells

Different phenotypes of ARPE-19 cells might associate with different biomechanical properties. To quantitatively analyze the biomechanical change in the living cells, the morphological data (including the 2D images, peak force error images, elasticity maps and 3D images) was obtained using AFM (Fig. **5a**). The surface roughness (Ra and Rq) was used to statistically characterize changes in cell topography. Compared with control group, the roughness of Y-27632-treated ARPE-19 cells (Ra: 41.04±1.63nm *vs.* 24.41±0.75nm, *P*<0.01; Rq: 51.56±2.03nm *vs.* 30.81±0.95nm, *P*<0.01) decreased showing a significant difference and these results are shown in Fig. **5b** and **5c**. Consistent with 3D images, the corrugations of cell surface were more evident in the control group in the peak force error images. After 48h of treatment with 30μM Y-27632, cell elasticity was also changed. Compared with control group, Young's modulus of Y-27632-treated cells (16.66±0.83KPa *vs.*

32.55±1.48KPa, *P*<0.01) increased, showing a significant difference, and the result is shown in Fig. **5d**.

3.4. Y-27632 Reorganizes Cytoskeleton of ARPE-19 Cells

Cell morphology and biomechanical property were determined by the cytoskeleton [37]. ROCK pathway inhabitation had been shown to reduce actin stress fibers formation and myosin phosphorylation [38]. Indeed, we found that Y-27632 converted ARPE-19 cells from rounded to an elongated shape and decreased roughness of ARPE-19 cells membrane, suggesting that the inhibition of ROCK pathway might reorganize the cytoskeleton.

Cytoskeleton morphology was illustrated after being exposed to Y-27632 exhibiting characteristic alterations including aggregation and distribution of microfilaments (MFs; Phalloidin) and microtubules (MTs; β -tubulin)
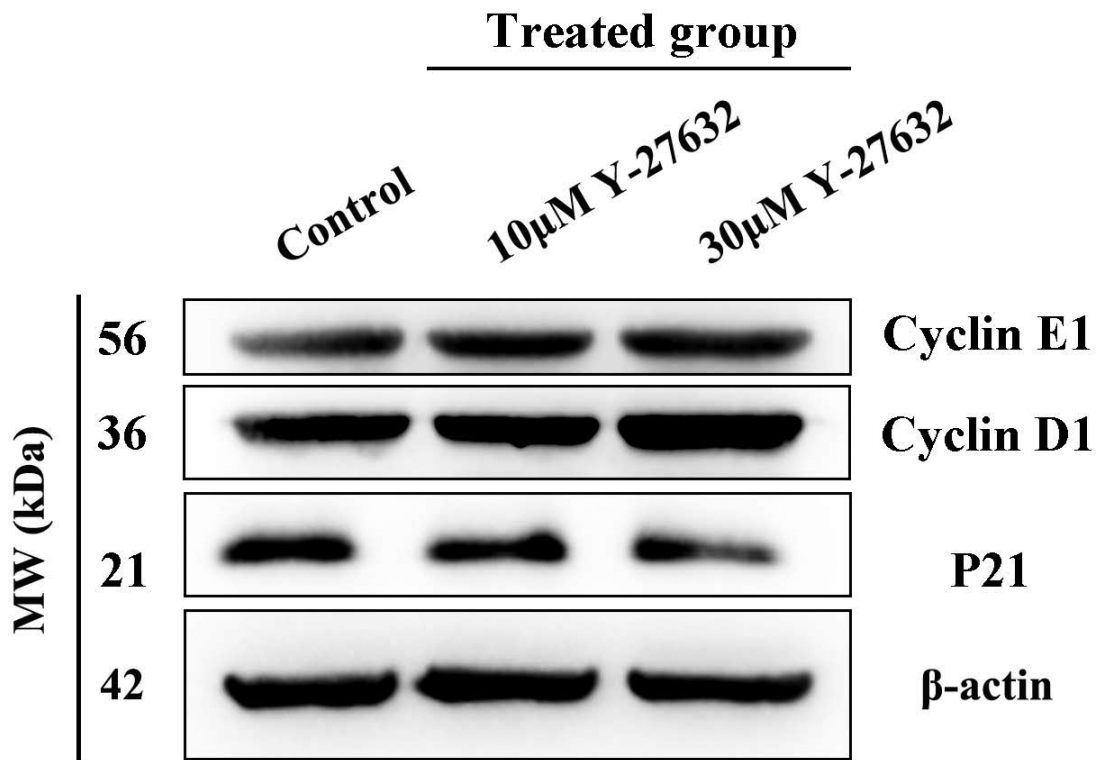
Fig. (3). The effect of ROCK inhibitor on cell cycle. ARPE-19 cells were treated with 10μM/30μM Y-27362 for 48h. Western blot was performed to probe for cyclin E1 (56 kDa), cyclin D1 (36 kDa), and P21 (21 kDa). β-actin (42 kDa) was used as an internal control.
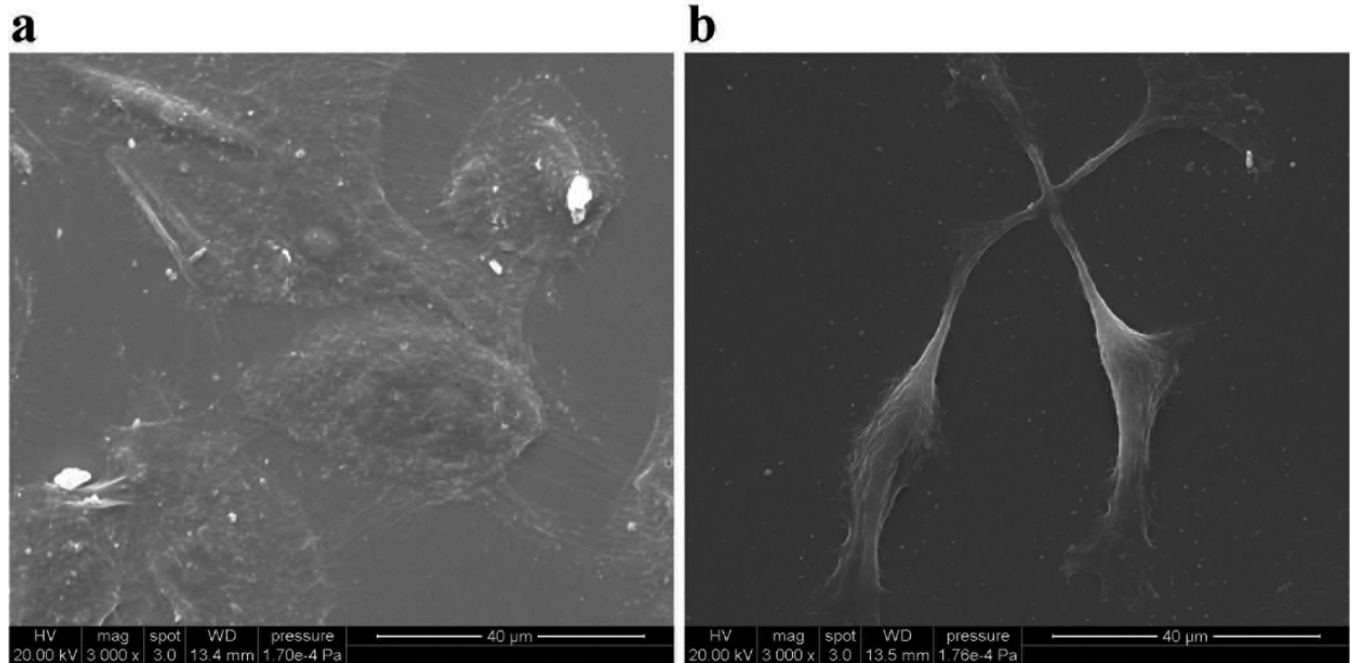
Fig. (4). The phenotype images of ARPE-19 cells using scanning electron microscopy. (**a**) Control cells show round up and had a typical polygonal appearance. (**b**) ARPE-19 cells treated with 30μM Y-27632 show elongation in shape. Scale bar: 40μm.
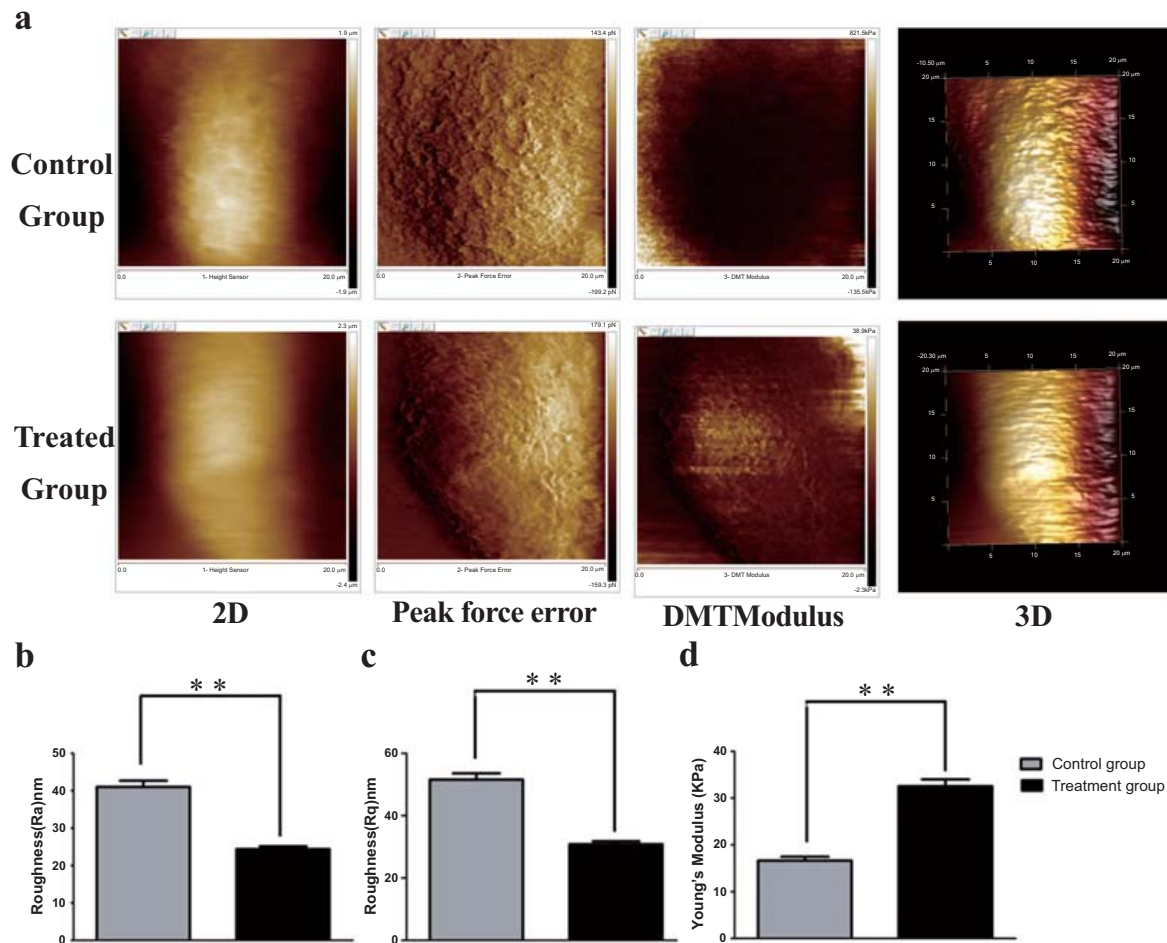
Fig. (5). Y-27632 Alter Biomechanical Properties of ARPE-19 Cells. Representative 2D images (column 1), peak force error images (column 2) and Young's modulus maps (column 3) as well as 3D images (column 4) of untreated and Y-27632 treated living ARPE-19 cells showing structural changes in local areas (**a**). (**b**) The arithmetic average roughness (Ra) values of ARPE-19 cells without and with of Y-27632 treatment (30µM) for 48 h. (**c**) The root-mean-square roughness (Rq) values of ARPE-19 cells without and with of Y-27632 treatment (30µM) for 48 h. (**d**) The Young's modulus values of ARPE-19 cells without and with Y-27632 treatment (30µM) for 48 h. N ≥ 15. Data represent the mean ± S.D. **P<0.01, n=3. Scale bar: 5µm.

(Fig. **6**). Normally, the cells exhibited a clear distribution of MFs and MTs, which possessed a dense cortical layer and an isotropic network in the cytoplasm. However, after 30µM Y-27632 treatment for 48h, the obvious reorganization of MFs and MTs with elongated shape was observed. In order to determine whether Y-27632 could induce epithelial–mesenchymal transition (EMT), we detected EMT markers. As compared to the expression level of the epithelial marker E-cadherin, fibrotic markers α-SMA and vimentin in control group, we found that the expression level of E-cadherin, α-SMA and vimentin remained unchanged in treated group (Fig. **7**).

4. DISCUSSION

In this study, we characterized the biomechanical properties in RPE cells after Y-27632 treatment using AFM for the first time. After being treated with Y-27632, the proliferation rate was significantly increased while apoptosis rate was significantly decreased. In addition, the roughness of RPE cells was significantly decreased

whereas Young's modulus of RPE cells significantly increased. Moreover, the cytoskeleton underwent reorganization after treated with Y-27632. These data indicated that Y-27632 may promote proliferation and inhibit apoptosis of RPE cells through changing the cell membrane properties as well as reorganizing cytoskeleton.

It is worth mentioning that ROCK activity inhibition leads to pro-apoptotic or pro-survival in a cell-type dependent manner. Most of the cancer studies supported the idea that inhibition of ROCK pathway suppressed cell cycle progression such as non-small cell lung cancer, bladder cancer and melanoma [39-41]. The underlying mechanism might be Rho/ROCK signaling which regulated the G1/S progression and DNA synthesis in fibroblast [42]. In addition, ROCK inhibitor Y-27632 was shown to be involved in p53-mediated apoptosis in hemangioma cells [43]. However, ROCK inhibitor, Y-27632, was also found to promote limbal epithelial cell proliferation through increasing S-phase cells [44]. Y-27632 was also shown
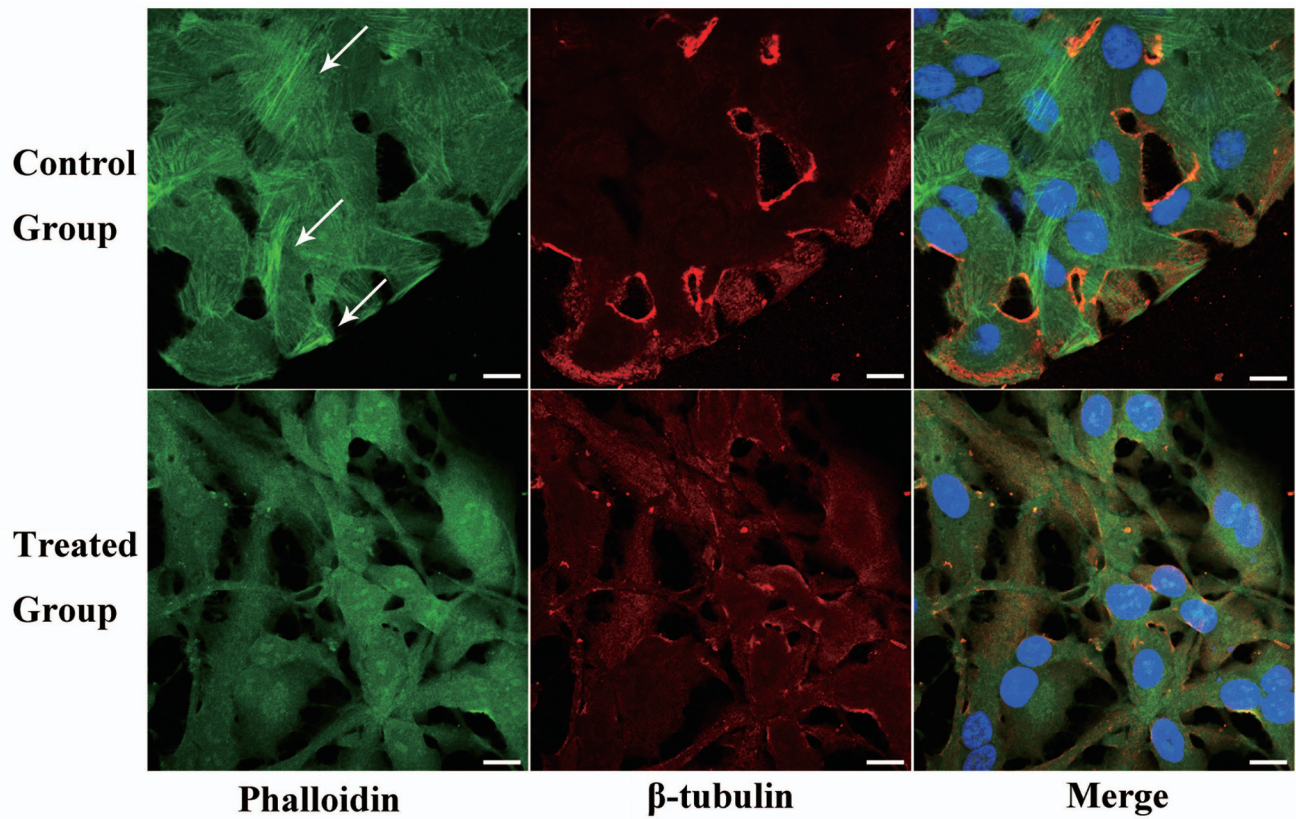
Fig. (6). The effect of ROCK inhibitor Y-27632 on microfilament (MF) and microtubule (MT) structure of ARPE-19 cells. ARPE-19 cells treated with/without 30µM Y-27632 for 48h were probed for MFs (Phalloidin, green), MTs (β-tubulin, red), and Hoechst (blue). Control group showed normal MFs (white arrows) and MTs distribution in ARPE-19 cells (0µM Y-27632 treatment). Treated group showed the obvious reorganization of MFs and the MTs in ARPE-19 cells (30µM Y-27632 treatment). Scale bar: 10µm.
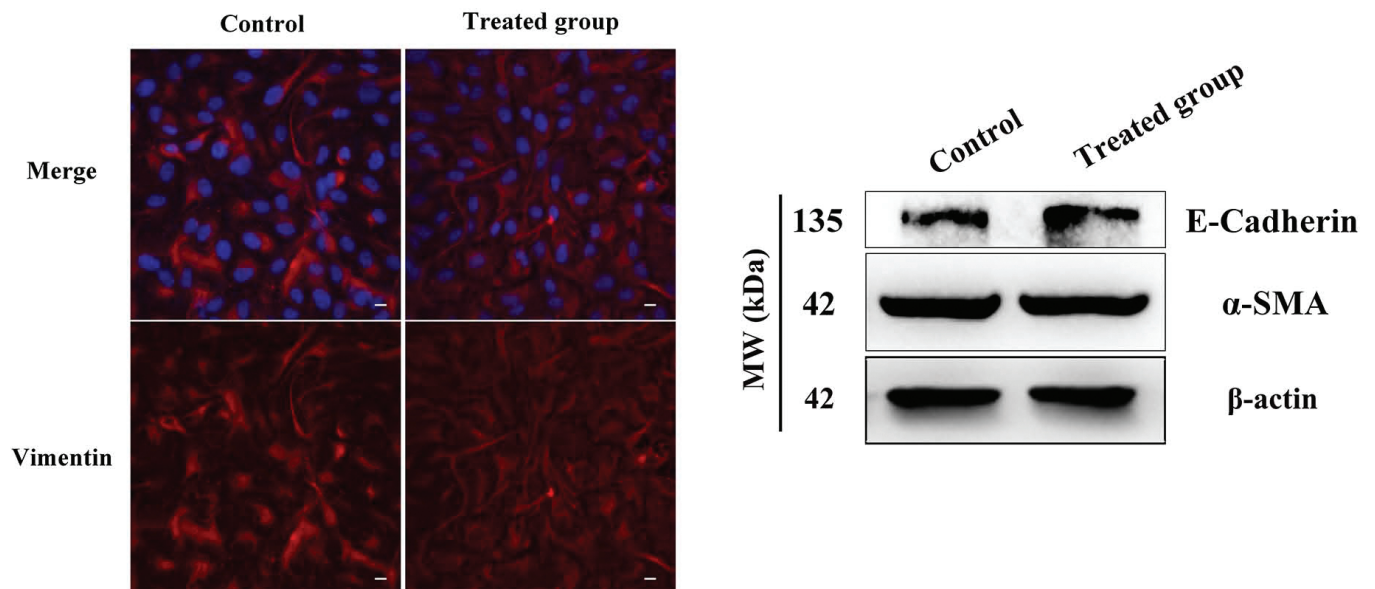
Fig. (7). ROCK inhibitor Y-27632 does not induce epithelial-mesenchymal transition (EMT) of ARPE-19 cells. (**a**) ARPE-19 cells treated with/without 30µM Y-27632 for 48h. Cells were probed for Vimentin (red) and Hoechst (blue). Scale bar: 10µm. (**b**) ARPE-19 cells treated with/without 30µM Y-27632 for 48h. Western blot analysis was performed to probe for E-Cadherin (135 kDa), and α-SMA (42 kDa). β-actin (42 kDa) was used as an internal control.

to deregulate P27 and upregulate the expression of cyclin D *via* PI3-kinase signaling to promote proliferation in corneal endothelial cells [45]. Moreover, ROCK inhibition was shown to enhance the survival of dissociated human embryonic stem cells [16]. Consistently, our result showed that Y-27632 promoted cell cycle progression through upregulating cyclin E1, cyclin D1 and downregulating P21.

Different cell types in different physiological conditions possess a unique cell membrane structure with specific biomechanical properties. In our study, by using AFM to analyze cell membrane biomechanical properties, we found that cell elasticity was significantly altered with the treatment of 30µM Y-27632 as the Young's modulus of treatment group showing significant upregulation. Consistently, Abidine *et al.*, also found that Y-27632 increased the plateau modulus of bladder cancer cell [46]. Recently, growing evidence suggests that the mechanical properties of the cell are closely related to cell proliferation, apoptosis, migration and adhesion. For example, Artesunate could inhibit the proliferation and migration of human glioma SHG44 cells by decreasing elasticity force or increasing adhesive force [47]. Consistently, Sodium nitroprusside (SNP)-induced apoptosis by decreasing cell elasticity in chondrocytes. Moreover, the biomechanical changes induced by SNP occurred before morphological changes, indicating that the cellular mechanical properties may be a more sensitive indicator of cell function [48].

Changes in the cell membrane may affect the signal transportation and subsequently, influence the cell cytoskeleton and survival [49]. Our study showed that Y-27632 treatment leads to the reorganization of MFs and MTs as well as the elongated shape of the cell. Known as an actin cytoskeletal organization regulator, ROCK participated in actin stress fiber formation and focal adhesion [50]. Changes in actomyosin structure might subsequently influence cell contractility, cell adhesion, cell migration and cell morphogenesis [12, 50]. In addition, the reorganization of cytoskeleton might influence chromosome stability and cell proliferation [51]. Further study is needed to reveal the underlying molecular mechanisms as well as the specific effects on the RPE cells due to changes in biomechanical properties.

It has been previously established that specific inhibition of the ROCK pathway might have a therapeutic benefit for the prevention of various vitreoretinal interface diseases especially PVR [21]. In this study, we investigated the role of ROCK signaling by utilizing its inhibitor Y-27632 which caused multiple changes in ARPE-19 cells. Further *in vivo* experiments are needed to evaluate its therapeutic effect and safety for clinical application.

CONCLUSION

In summary, our study revealed that the ROCK inhibitor Y-27632 induced increased proliferation, decreased apoptosis and changes in biophysical properties as well as the cytoskeletal reorganization of ARPE-19 cells. The reorganization of the cytoskeletons combined with cell elongation is likely to bring changes in cellular elasticity and morphology. These results may provide insightful understanding and the reference value to the application of Y-27632 in RPE degeneration diseases.

ABBREVIATIONS

RPE	=	Retinal pigment epithelium
PVR	=	Proliferative vitreoretinopathy
AMD	=	Age-related macular degeneration
AFM	=	Atomic force microscopy
LSCM	=	Laser scanning confocal microscope
Ra	=	Arithmetic average roughness
Rq	=	Root-mean-square roughness
RT	=	Room temperature
MFs	=	Microfilaments
MTs	=	Microtubules

ETHICS APPROVAL AND CONSENT TO PARTICIPATE

Not applicable.

HUMAN AND ANIMAL RIGHTS

No Animals/Humans were used for studies that are base of this research.

CONSENT FOR PUBLICATION

Not applicable.

CONFLICT OF INTEREST

The authors declare no conflict of interest, financial or otherwise.

REFERENCES

[1]   Strauss O. The retinal pigment epithelium in visual function. Physiol Rev 2005; 85(3): 845-81.
[2]   Sparrow JR, Hicks D, Hamel CP. The retinal pigment epithelium in health and disease. Curr Mol Med 2010; 10(9): 802-23.
[3]   Walia S, Fishman GA. Natural history of phenotypic changes in Stargardt macular dystrophy. Ophthalmic Genet 2009; 30(2): 63-8.

[4]   Bovolenta P, Cisneros E. Retinitis pigmentosa: cone photoreceptors starving to death. Nat Neurosci 2009; 12(1): 5-6.

[5]   Zhan J, He J, Zhou Y, *et al*. Crosstalk Between the Autophagy-Lysosome Pathway and the Ubiquitin-Proteasome Pathway in Retinal Pigment Epithelial Cells. Curr Mol Med 2016; 16(5): 487-95.

[6]   Lingor P, Tonges L, Pieper N, *et al*. ROCK inhibition and CNTF interact on intrinsic signalling pathways and differentially regulate survival and regeneration in retinal ganglion cells. Brain 2008; 131(Pt 1): 250-63.

[7]   Wang Y, Shen D, Wang VM, *et al*. Enhanced apoptosis in retinal pigment epithelium under inflammatory stimuli and oxidative stress. Apoptosis 2012; 17(11): 1144-55.

[8]   Jang KH, Do YJ, Son D, Son E, Choi JS, Kim E. AIF-independent parthanatos in the pathogenesis of dry age-related macular degeneration. Cell Death Dis 2017; 8(1): e2526.

[9]   Leung T, Manser E, Tan L, Lim L. A novel serine/threonine kinase binding the Ras-related RhoA GTPase which translocates the kinase to peripheral membranes. J Biol Chem 1995; 270(49): 29051-4.

[10]   Leung T, Chen XQ, Manser E, Lim L. The p160 RhoA-binding kinase ROK alpha is a member of a kinase family and is involved in the reorganization of the cytoskeleton. Mol Cell Biol 1996; 16(10): 5313-27.

[11]   Nakagawa O, Fujisawa K, Ishizaki T, Saito Y, Nakao K, Narumiya S. ROCK-I and ROCK-II, two isoforms of Rho-associated coiled-coil forming protein serine/threonine kinase in mice. Febs Lett 1996; 392(2): 189-93.

[12]   Riento K, Ridley AJ. Rocks: multifunctional kinases in cell behaviour. Nat Rev Mol Cell Biol 2003; 4(6): 446-56.

[13]   Masamune A, Kikuta K, Satoh M, Satoh K, Shimosegawa T. Rho kinase inhibitors block activation of pancreatic stellate cells. Br J Pharmacol 2003; 140(7): 1292-302.

[14]   Moore M, Marroquin BA, Gugliotta W, Tse R, White SR. Rho kinase inhibition initiates apoptosis in human airway epithelial cells. Am J Respir Cell Mol Biol 2004; 30(3): 379-87.

[15]   Cechin SR, Dunkley PR, Rodnight R. Signal transduction mechanisms involved in the proliferation of C6 glioma cells induced by lysophosphatidic acid. Neurochem Res 2005; 30(5): 603-11.

[16]   Watanabe K, Ueno M, Kamiya D, *et al*. A ROCK inhibitor permits survival of dissociated human embryonic stem cells. Nat Biotechnol 2007; 25(6): 681-6.

[17]   Braam SR, Nauw R, Ward-van OD, Mummery C, Passier R. Inhibition of ROCK improves survival of human embryonic stem cell-derived cardiomyocytes after dissociation. Ann N Y Acad Sci 2010; 1188: 52-7.

[18]   Bao W, Hu E, Tao L, *et al*. Inhibition of Rho-kinase protects the heart against ischemia/reperfusion injury. Cardiovasc Res 2004; 61(3): 548-58.

[19]   Xiang SY, Vanhoutte D, Del RD, *et al*. RhoA protects the mouse heart against ischemia/reperfusion injury. J Clin Invest 2011; 121(8): 3269-76.

[20]   Okumura N, Ueno M, Koizumi N, *et al*. Enhancement on primate corneal endothelial cell survival in vitro by a ROCK inhibitor. Invest Ophthalmol Vis Sci 2009; 50(8): 3680-7.

[21]   Zheng Y, Bando H, Ikuno Y, *et al*. Involvement of rho-kinase pathway in contractile activity of rabbit RPE cells in vivo and in vitro. Invest Ophthalmol Vis Sci 2004; 45(2): 668-74.

[22]   Lu Z, Overby DR, Scott PA, Freddo TF, Gong H. The mechanism of increasing outflow facility by rho-kinase inhibition with Y-27632 in bovine eyes. Exp Eye Res 2008; 86(2): 271-81.

[23]   Van de Velde S, Van Bergen T, Sijnave D, *et al*. AMA0076, a novel, locally acting Rho kinase inhibitor, potently lowers intraocular pressure in New Zealand white rabbits with minimal hyperemia. Invest Ophthalmol Vis Sci 2014; 55(2): 1006-16.

[24]   Hein TW, Rosa RJ, Yuan Z, Roberts E, Kuo L. Divergent roles of nitric oxide and rho kinase in vasomotor regulation of human retinal arterioles. Invest Ophthalmol Vis Sci 2010; 51(3): 1583-90.

[25]   Narimatsu T, Ozawa Y, Miyake S, *et al*. Disruption of cell-cell junctions and induction of pathological cytokines in the retinal pigment epithelium of light-exposed mice. Invest Ophthalmol Vis Sci 2013; 54(7): 4555-62.

[26]   Nakamura Y, Hirano S, Suzuki K, Seki K, Sagara T, Nishida T. Signaling mechanism of TGF-beta1-induced collagen contraction mediated by bovine trabecular meshwork cells. Invest Ophthalmol Vis Sci 2002; 43(11): 3465-72.

[27]   Kramer A, Liashkovich I, Oberleithner H, Ludwig S, Mazur I. Apoptosis leads to a degradation of vital components of active nuclear transport and a dissociation of the nuclear lamina. Proc Natl Acad Sci U S A 2008; 105(32): 11236-41.

[28]   Jin H, Liang Q, Chen T, Wang X. Resveratrol protects chondrocytes from apoptosis via altering the ultrastructural and biomechanical properties: an AFM study. PLoS One 2014; 9(3): e91611.

[29]   Nishiyama A, Yao L, Fan Y, *et al*. Involvement of aldosterone and mineralocorticoid receptors in rat mesangial cell proliferation and deformability. Hypertension 2005; 45(4): 710-6.

[30]   Hu E, Lee D. Rho kinase as potential therapeutic target for cardiovascular diseases: opportunities and challenges. Expert Opin Ther Targets 2005; 9(4): 715-36.

[31]   Shi X, Zhang X, Xia T, Fang X. Living cell study at the single-molecule and single-cell levels by atomic force microscopy. Nanomedicine (Lond) 2012; 7(10): 1625-37.

[32]   Saha SK, Khuda-Bukhsh AR. Berberine alters epigenetic modifications, disrupts microtubule network, and modulates HPV-18 E6-E7 oncoproteins by targeting p53 in cervical cancer cell HeLa: a mechanistic study including molecular docking. Eur J Pharmacol 2014; 744: 132-46.

[33]   Zhang L, Yang F, Cai JY, Yang PH, Liang ZH. In-situ detection of resveratrol inhibition effect on epidermal growth factor receptor of living MCF-7 cells by Atomic Force Microscopy. Biosens Bioelectron 2014; 56: 271-7.

[34]   Fang Z, Jiang C, Tang J, *et al*. A comprehensive analysis of membrane and morphology of erythrocytes from patients with glucose-6-phosphate dehydrogenase deficiency. J Struct Biol 2016; 194(3): 235-43.

[35]   Fang Z, Jiang C, Feng Y, *et al*. Effects of G6PD activity inhibition on the viability, ROS generation and mechanical properties of cervical cancer cells. Biochim Biophys Acta 2016; 1863(9): 2245-54.

[36]   Lundberg AS, Weinberg RA. Functional inactivation of the retinoblastoma protein requires sequential modification by at least two distinct cyclin-cdk complexes. Mol Cell Biol 1998; 18(2): 753-61.

[37]   Fuchs E, Cleveland DW. A structural scaffolding of intermediate filaments in health and disease. Science 1998; 279(5350): 514-9.

[38]   Mokady D, Meiri D. RhoGTPases - A novel link between cytoskeleton organization and cisplatin resistance. Drug Resist Updat 2015; 19: 22-32.

[39]   Vigil D, Kim TY, Plachco A, *et al*. ROCK1 and ROCK2 are required for non-small cell lung cancer anchorage-independent growth and invasion. Cancer Res 2012; 72(20): 5338-47.

[40]   Jiang L, Wen J, Luo W. Rhoassociated kinase inhibitor, Y27632, inhibits the invasion and proliferation of T24 and 5367 bladder cancer cells. Mol Med Rep 2015; 12(5): 7526-30.

[41]   Spencer C, Montalvo J, McLaughlin SR, Bryan BA. Small molecule inhibition of cytoskeletal dynamics in melanoma tumors results in altered transcriptional expression patterns of key genes involved in tumor initiation and progression. Cancer Genomics Proteomics 2011; 8(2): 77-85.

[42]   Olson MF, Ashworth A, Hall A. An essential role for Rho, Rac, and Cdc42 GTPases in cell cycle progression through G1. Science 1995; 269(5228): 1270-2.

[43]   Qiu MK, Wang SQ, Pan C, *et al*. ROCK inhibition as a potential therapeutic target involved in apoptosis in hemangioma. Oncol Rep 2017; 37(5): 2987-93.

[44]   Sun CC, Chiu HT, Lin YF, Lee KY, Pang JH. Y-27632, a ROCK Inhibitor, Promoted Limbal Epithelial Cell Proliferation

and Corneal Wound Healing. PLoS One 2015; 10(12): e144571.

[45]   Okumura N, Nakano S, Kay EP, *et al*. Involvement of cyclin D and p27 in cell proliferation mediated by ROCK inhibitors Y-27632 and Y-39983 during corneal endothelium wound healing. Invest Ophthalmol Vis Sci 2014; 55(1): 318-29.

[46]   Abidine Y, Laurent VM, Michel R, Duperray A, Verdier C. Local mechanical properties of bladder cancer cells measured by AFM as a signature of metastatic potential. Eur Phys J Plus 2015; 130(10): 202.

[47]   Lian S, Shi R, Huang X, *et al*. Artesunate attenuates glioma proliferation, migration and invasion by affecting cellular mechanical properties. Oncol Rep 2016; 36(2): 984-90.

[48]   Jin H, Liang Q, Chen T, Wang X. Resveratrol protects chondrocytes from apoptosis via altering the ultrastructural

and biomechanical properties: an AFM study. PLoS One 2014; 9(3): e91611.

[49]   Sato K, Adachi T, Ueda D, Hojo M, Tomita Y. Measurement of local strain on cell membrane at initiation point of calcium signaling response to applied mechanical stimulus in osteoblastic cells. J Biomech 2007; 40(6): 1246-55.

[50]   Julian L, Olson MF. Rho-associated coiled-coil containing kinases (ROCK): structure, regulation, and functions. Small GTPases 2014; 5: e29846.

[51]   Saunders WS, Shuster M, Huang X, *et al*. Chromosomal instability and cytoskeletal defects in oral cancer cells. Proc Natl Acad Sci U S A 2000; 97(1): 303-8.